Numerical investigation of the linear response of a viscous liquid sheet

N. Alleborn, H. Raszillier

Lehrstuhl für Strömungsmechanik, Universität Erlangen–Nürnberg,
Cauerstr. 4, D–91058 Erlangen, Germany

Abstract

In this paper the propagation of disturbance signals in a uniformly thin viscous liquid sheet of infinite extent which is in contact with a passive ambient medium is investigated. The disturbances considered are induced by local external pressure perturbations moving on the sheet interfaces. The tool of analysis is the Fourier-Laplace transform of the linearized perturbation equations, and the inverse Fourier-Laplace transform for the numerical reconstruction of the amplitude of the interface deflections. Symmetric (varicose) and antisymmetric (sinuous) disturbances are investigated in the long time limit by numerical signal evaluation. The exact disturbance responses are compared with their longwave approximations.

1 Introduction

Thin viscous liquid sheets are sensitive to external disturbances, such as pressure fluctuations along their interfaces. In liquid film coating, falling sheets of this kind are used to deposit a thin and uniform liquid layer on moving substrates. In this and other applications, maintaining a uniform undisturbed liquid sheet is desired. Due to the rather low relative velocity of the sheet and the low density and viscosity of the ambient medium, the response of the sheet to disturbances is essentially dominated by viscosity, capillarity and inertia of the sheet itself, while the interaction with the ambient medium can be reduced to external pressure distributions acting on the free surfaces of the sheet. Further more, the elongation of a sheet falling under gravity may be ignored for small Bond number $Bo = \rho g h^2/\gamma$, with the density ρ, the gravitational acceleration g, the surface tension γ and the (local) sheet thickness h.

In this framework, the unperturbed plane liquid sheet of infinite extent and constant thickness may be considered appropriately in its rest frame. In a linear stability analysis for this configuration Lin et al. [9, 10] showed that the sheet is stable against small perturbations. Local variations of the external pressure will therefore generate a surface deflection coupled with a fluid flow within the liquid sheet, resulting in a wave motion, which separates, due to symmetry, into so called sinuous and varicose modes.

Lin and Roberts [11] investigated waves on falling sheets experimentally for aqueous glycerine and gelatine solutions with viscosities more than one order of magnitude higher than pure water, and identified sinuous and varicose modes of curtain waves, generated by a solid obstacle puncturing the falling liquid sheet. De Luca and Costa [8] presented an asymptotic expansion for the surface deflection generated by a disturbance on an inviscid falling sheet and compared the wave patterns with experiments for low viscous sheets.

Recently, an investigation of the response of thin *viscous* liquid sheets to instantaneous and persistent (oscillating) point and line sources has been undertaken in [4, 12, 13] in the framework of long wave approximation. In the present paper, the long time asymptotic response to steady persistent perturbations is investigated numerically both for varicose and sinuous perturbation forms, extending earlier work presented in [3, 5].

2 Formulation of the Problem

The linear response of a uniform viscous liquid sheet (of density ρ, kinematic viscosity ν, surface tension γ) of infinite extent to localized pressure disturbances will be investigated. Fig. 1 (a) shows

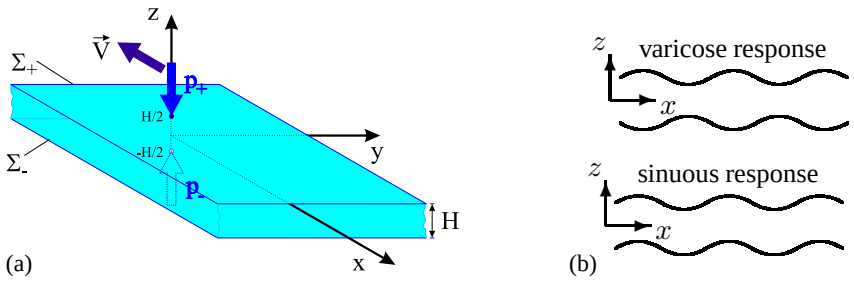

Figure 1: Sketch of a thin viscous liquid sheet (a), perturbation modes (b).

a sketch of the sheet with a *passive* ambient medium adjacent to it, which exerts the pressure distributions $p_\pm(\vec{x}_\parallel, t)$ on the sheet interfaces $\Sigma_\pm$, with the twodimensional vector in the xy–plane $\vec{x}_\parallel = (x, y)$. For constant pressures $p_+ = p_- = p_0$, flat interfaces $h_\pm = \pm H/2$, a constant velocity profile $\vec{u}_0 = U_0\vec{e}_x$ and a constant pressure $p = p_0$ in the sheet provide a solution of the governing equations and boundary conditions. This basic flow may be considered in the rest frame of the fluid, i.e. with $U_0 = 0$. The pressure p_0 may be considered as reference (i.e. as $p_0 = 0$).

Small local deviations of $p_\pm$ from p_0 induce a flow in the sheet, causing small fluctuations $\eta_\pm$ of the interfaces around its basic state: $h_\pm = \pm(H/2+\eta_\pm)$, coupled with small velocity and pressure fluctuations, $\vec{u}_p$ and p_p, respectively. In Fig. 1 (a) (localized) pressure disturbances moving with constant velocity $\vec{V}$ act on the interfaces. A reflection symmetry of the basic state with respect to the plane $z = 0$ allows to consider *varicose* perturbations, that act symmetrically on the interfaces ($p_- = p_+$), and *sinuous* perturbations, that act antisymmetrically ($p_- = -p_+$), separately, cf. Fig. 1 (b), with the response amplitudes $\eta_- = \eta_+$ and $\eta_- = -\eta_+$, respectively.

The linearized perturbation equations are conveniently solved by a twodimensional Fourier–Laplace transformation in the xy-plane and in time, see [4] for details. In the sequel only twodimensional vectors will be considered and the subscript $\parallel$ will be dropped accordingly. The amplitudes η_+ of the varicose and sinuous interface deformations, $\eta_{v,s}$, are obtained by an inverse Fourier–Laplace transform as

$$\eta_{v,s}(\vec{x}, t) = -\frac{1}{2\pi}\int d\vec{k}\, e^{i\vec{k}\cdot\vec{x}}\ \frac{1}{2\pi i}\int_{c-i\infty}^{c+i\infty} d\omega\ e^{\omega t}\ \frac{k\,\tilde{\mathcal{P}}(\vec{k},\omega)}{D_{v,s}(k,\omega)}\,, \quad c > 0\,, \tag{1}$$

from the linear perturbation equations, cf. [4], stated here already in dimensionless terms by normalizing lengths by $H/2$, time by $H^2/(4\nu)$ and pressure by $4\rho\nu^2/H^2$. $\tilde{\mathcal{P}}(\vec{k},\omega)$ denotes the Fourier–Laplace transform of the pressure disturbance $p_+(\vec{x}, t)$ and $D_{v,s}(k,\omega)$ the varicose and sinuous dispersion function, respectively:

$$D_v(k,\omega) = \Gamma^2 k^3 + (k^2+l^2)^2\coth(k) - 4k^3 l\coth(l)\,, \tag{2}$$

$$D_s(k,\omega) = \Gamma^2 k^3 + (k^2+l^2)^2\tanh(k) - 4k^3 l\tanh(l)\,, \tag{3}$$

with the twodimensional wave vector $\vec{k}$, $k = |\vec{k}|$ and $l^2 = k^2 + \omega$ and with the characteristic number of the sheet

$$\Gamma = \sqrt{\gamma H/(2\rho\nu^2)}\,. \tag{4}$$

The singularities of the integrand in eq. (1), the zero curves $\omega = \omega(k)$ of $D_{v,s}(k,\omega) = 0$, lie in the left half of the complex ω–plane, i.e. the response modes of the sheet are absorptive [13]. A qualitative analysis of the varicose and sinuous spectra of the sheet has been performed in [13]; it revealed that each one consists of infinitely many branches $\omega_\alpha(k)$, of which only two are "soft", with $\lim_{k\to 0} \omega_\alpha(k) = 0$, while the remaining are "hard", i.e. bound away from $\omega = 0$. A quantitative insight into the structure of the sheet spectrum will be obtained by a numerical parameter continuation method, cf. [6].

3 Results and Discussion

3.1 Disturbance and Response

A persistent localized disturbance $p_+(\vec{x},t) = P(\vec{x} + \vec{V}t)\,\theta(t)$, moving with velocity $\vec{V}$ in the rest frame of the sheet and acting for $t > 0$, is considered. A formula for the response of the sheet in the long time limit ($t \to \infty$) is then evaluated numerically. It is convenient to analyze the response in the rest frame of the perturbation, i.e. to carry out the transformation $\vec{X} = \vec{x} + \vec{V}t$. The spatial distribution of the pressure, $P(\vec{X})$, is represented as $P(\vec{X}) = P_0\, f(\vec{X})$, with a shape function $f(\vec{X})$.

For varicose pressure disturbances the sheet is statically equilibrated for any pressure distribution, i.e. the total force exerted by the ambient pressure on the sheet vanishes, since by definition $p_+ = p_-$. For the investigation of the varicose response a normalized Gaussian shape function f_G, with its Fourier transform $\tilde{f}_G$,

$$f_G(\vec{X},a) = \frac{1}{a^2\pi}\, e^{-\frac{r^2}{a^2}}\,, \qquad \tilde{f}_G(\vec{k},a) = \frac{1}{2\pi}\, e^{-\frac{k^2a^2}{4}}\,, \tag{5}$$

with $r = \|\vec{X}\| = \sqrt{X^2+Y^2}$ and $\int_{-\infty}^{\infty}\int_{-\infty}^{\infty} f_G(\vec{X},a)\,dX\,dY = 1$, will be used in the following sections.

A sinuous pressure disturbance, with $p_+ = -p_-$, however, has to be chosen in such a way that the sheet is statically equilibrated, i.e. $\iint p_+(\vec{x},t)d\vec{x} = 0$. In this paper, the form function $f_0 = -\Delta f_G$, with its Fourier transform $\tilde{f}_G$, is chosen for such a distribution:

$$f_0(\vec{X},a) = \frac{4}{a^4\pi}\left(1 - \frac{r^2}{a^2}\right) e^{-\frac{r^2}{a^2}}\,, \qquad \tilde{f}_0(\vec{k},a) = \frac{k^2}{2\pi}\, e^{-\frac{k^2a^2}{4}}\,. \tag{6}$$

In the limit $t \to \infty$ the reponse signal becomes:

$$\eta_{s,v\,\infty}(\vec{X}) = -\frac{P_0}{2\pi}\int_{-\infty}^{\infty}\int_{-\infty}^{\infty} d\vec{k}\, e^{i\vec{k}\cdot\vec{X}}\, \frac{k\,\tilde{f}(\vec{k})}{D_{s,v}(k, i\vec{k}\cdot\vec{V})}\,. \tag{7}$$

At large enough distances from the perturbing source, the two "soft" branches $\omega_{s,v\pm}(k)$, for which $\lim_{k\to 0} \omega_{s,v\pm}(k) = 0$, and even the long wave parts ($k \to 0$) of these branches, are expected to dominate the signals, cf. [4, 13]. The Fourier integral, eq. (7), will be evaluated numerically both for the exact dispersion functions of the sheet, eqs. (2)–(3), and for their long wave approximations by using the algorithm A698 [7] for adaptive multi-dimensional numerical integration, which has already been applied in [3] to this problem.

3.2 Signal Evaluation: Varicose Excitation

The long wave approximations of the *varicose* "soft" branches to lowest order, $\omega_{v\pm}(k) \approx \pm\sqrt{4-\Gamma^2}\,k^2 - 2k^2$, are *real* (i.e. purely absorptive) for $\Gamma^2 < 4$ and oscillatory (with complex conjugate dispersive parts) for $\Gamma^2 > 4$, cf. [12]. Fig. 2 shows part of the varicose spectrum derived numerically from eq. (2) for $\Gamma = 1$. Together with the two soft branches, denoted by ω_{v+} and ω_{v-}, respectively, the first three hard branches are shown in Fig. 2 (a); they are strongly damped compared to the soft modes. In Fig. 2 (b) the real parts of the soft branches $\omega_{v\pm}$, obtained nu-

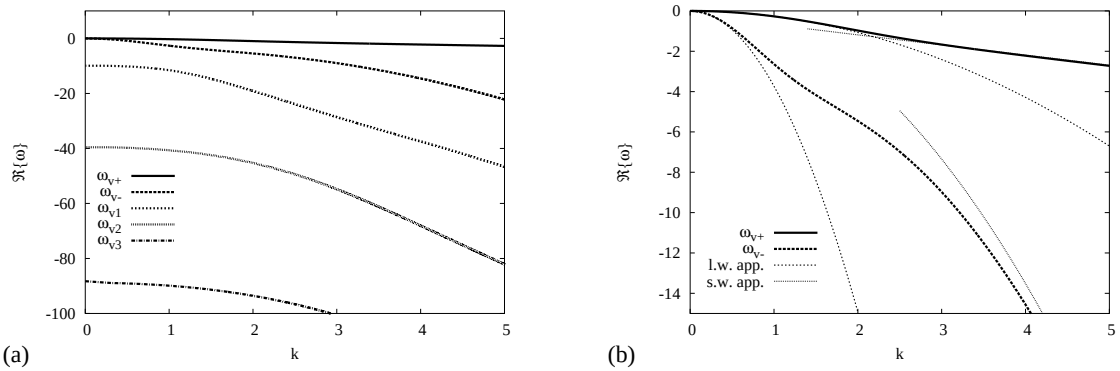

Figure 2: Real part $\Re(\omega)$ of the varicose spectrum for $\Gamma = 1$: soft and hard branches (a), magnified view of soft branches (b). Imaginary part $\Im(\omega) = 0$, "l.w.app" and "s.w.app" denote long wave and short wave approximation, respectively, cf. [13].

merically, are plotted and compared with the asymptotic approximations derived in [13] for long waves, $k \ll 1$, and short waves, $k \gg 1$, respectively.

In the lowest order of the long wave approximation an analytical expression for the response of the liquid sheet to a persistent point disturbance $p_e(\vec{X}, t) = P_e\delta(\vec{X})\theta(t)$ was presented in [4]. This analytic expression is ideally suited for the validation of the numerical evaluations of the signal integral (7). An inspection immediately shows, that the procedure of [4] can be extended straightforwardly to the derivation of an analytic form also for the excitation of Gaussian shape [1]. In Fig. 3 results of the numerical integration of eq. (7) are presented for $\Gamma = 1$ (left) and $\Gamma = 10$ (right) for a persistent varicose disturbance $p_+(\vec{X}, t) = P_0\, f_G(\vec{X}, 1/10)\,\theta(t)$, for the exact dispersion function, eq. (2), (curve (c) in Fig. 3), and its lowest order long wave approximation, (curve (b) in Fig. 3). The result for the numerical integration of eq. (7) with the long wave dispersion relation thereby agrees perfectly with the evaluation of analytical expression for the response to the Gaussian excitation [1], plotted as crosses (a) in Fig. 3. With increasing distance from the perturbation source, for $x \gg 4$, the analytical response amplitude in the long wave approximation approaches the response amplitude computed numerically with the exact dispersion function.

Since the dominant (long wave) varicose spectral modes are purely absorptive for $\Gamma \leq 2$, the response of the sheet to the pressure perturbation exhibits an aperiodic behaviour. For $\Gamma > 2$ the dominant modes are oscillatory. Fig. 4 indicates that the (analytical) location of the wave crests in the framework of long wave approximation for the excitation (5), derived along the lines of [4], coincides with the wave crests obtained numerically from eq. (7) for the exact dispersion relation at some distance downstream of the localized perturbation.

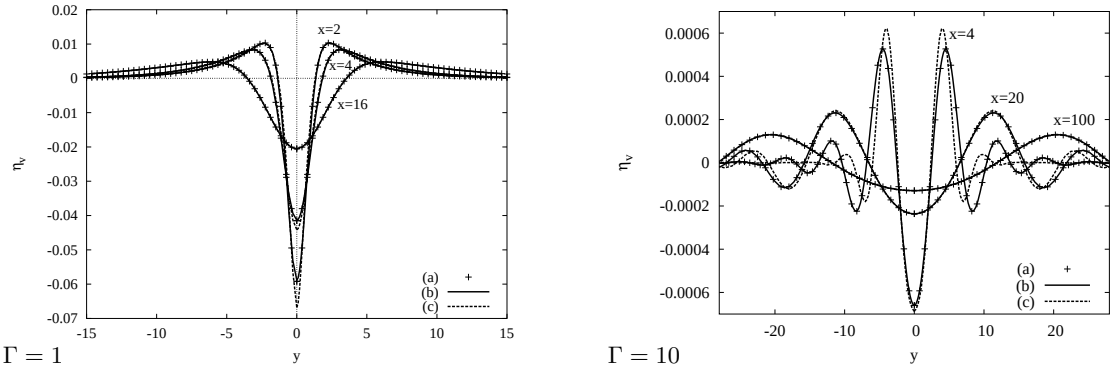

Figure 3: Disturbance amplitude $\eta_v(x, y)$ along the y–direction at different distances x from the source, for $\Gamma = 1$ (left) and $\Gamma = 10$ (right), with $V = 2\Gamma$ (rest frame of disturbance source). Analytic form of the lowest order longwave approximation of the varicose sheet response [1] (a), numerically evaluated signal with lowest order longwave dispersion function (b), and with the exact dispersion function (c).

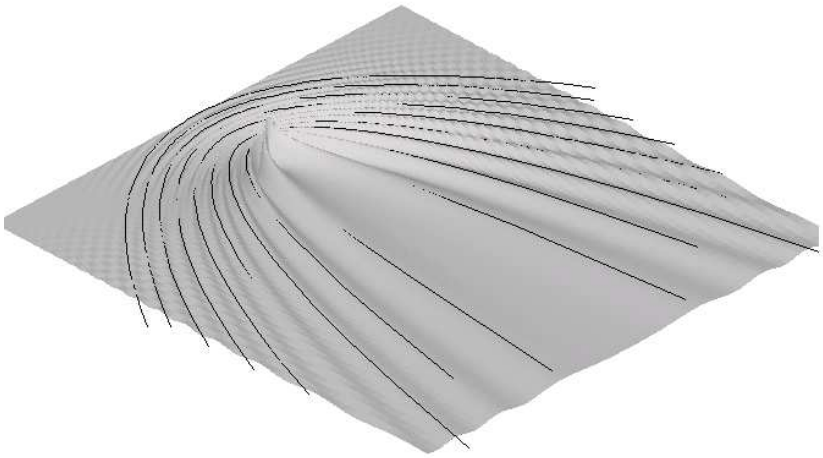

Figure 4: Response to a localized varicose disturbance ($a = 0.1$) for $\Gamma = 126.3, V = 1.319\Gamma$ (rest frame of disturbance). Contour lines (black): Location of the wave crests as computed by the long wave approximation, along the lines of [1, 4].

3.3 Complex Varicose Excitation: Superposition

In this section, a disturbance of a shape described by a superposition of Gaussians of the form $f_G(\vec{X} - \vec{X}_0, a)$, with $\vec{X}_0 = (X_0, Y_0)$ covering the rectangular region $[-l_x, l_x] \times [-l_y, l_y]$:

$$f_R(X,Y) = \frac{1}{16\, l_x\, l_y} \left(\text{erf}\left(\frac{X + l_x}{a}\right) + \text{erf}\left(\frac{l_x - X}{a}\right)\right) \cdot \left(\text{erf}\left(\frac{Y + l_y}{a}\right) + \text{erf}\left(\frac{l_y - Y}{a}\right)\right) \quad (8)$$

is considered in order to illustrate the response to a *distributed* source. It is a smoothed approximation of the step function

$$\theta_R(X,Y) = \frac{1}{4\, l_x\, l_y}\, (\theta(X + l_x) - \theta(X - l_x)) \cdot (\theta(Y + l_y) - \theta(Y - l_y)) \quad (9)$$

with the Heaviside function $\theta(x)$.

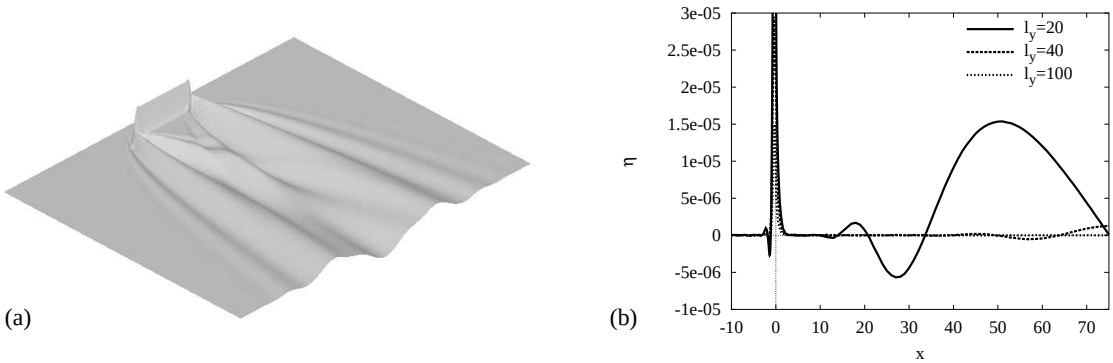

Figure 5: Response of the liquid sheet to a varicose pressure disturbance of width $l_x = 0.1, l_y = 20$ for $\Gamma = 10, V = 2\Gamma$, in the rest frame of the disturbance (a). Disturbance amplitude along the line $y = 0$ for different widths l_y, with $\Gamma = 10, V = 2\Gamma$ (b).

It causes, like the Gaussian shape function (5), an exponential suppression of the short wave lengths. Fig. 5 (a) shows the varicose response of the sheet to a blade shaped pressure disturbance with $l_x = 0.1, l_y = 20$. A straight wave crest is seen to build up in front of the perturbing source, perpendicularly to its motion. From the edges of the region of perturbation waves are generated, which merge some distance downstream in the wake of the source. In the immediate downstream vicinity of the source, a triangularly shaped area with practically vanishing amplitude develops. This area increases with increasing width l_y of the source of perturbation. In the limit $l_y \to \infty$ the source comes close to a line source, for which it was shown in [4] in the long wave limit that its downstream response amplitude is infinitesimally small, yet with a finite integral deflection value to compensate the upstream deflection amplitude as required by mass conservation. The response amplitude of the sheet along the line $y = 0$ is shown in Fig. 5 (b) for different widths l_y of the perturbation, indicating an area of small amplitude, that increases with $l_y \to \infty$ and approaches in the limit the line source response.

3.4 Signal Evaluation: Sinuous Excitation

Like the varicose part of the sheet spectrum, the sinuous spectrum consists of two soft branches, denoted by $\omega_{s\pm}$, and infinitely many hard branches $\omega_{s\alpha}$. Fig. 6 shows part of this spectrum derived numerically from the dispersion function (3), for $\Gamma = 1$: the real (absorptive) parts of the soft branches together with the first three hard branches $\omega_{s1,2,3}$, which are purely real and seen to be very strongly damped compared to the soft ones.

The lowest orders for the real (absorptive) and for the imaginary (dispersive) parts of the long wave approximation of the soft branches are given by [12, 13]

$$\omega_{s\pm}(k) \approx \pm i\,\Gamma\,k - \left(\frac{2}{3} + \frac{4}{15}\Gamma^2\right) k^4\,, \tag{10}$$

with the long wave sinuous dispersion function

$$D_s(k,\omega) = k\,(\omega - \omega_{s+})(\omega - \omega_{s-})\,. \tag{11}$$

The sinuous soft modes are *nondispersive* in the leading order, with a dimensionless phase speed $c_{ph} = |\Im\{\omega_{s\pm}\}|/k = \Gamma$. The lowest order *absorptive* term is $\propto k^4$. Compared with the leading

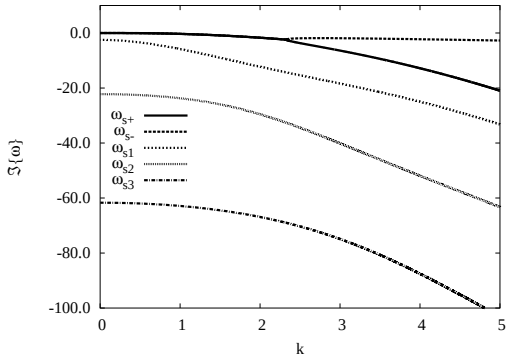

Figure 6: Real part $\Re(\omega)$ of the spectrum for $\Gamma = 1$: sinuous modes.

order long wave approximation of the varicose soft branches, Fig. 2, the approximation of the real (absorptive) part of the sinuous soft branches by the leading order long wave asymptotics is less accurate, as a plot of these branches in Fig. 7 indicates.

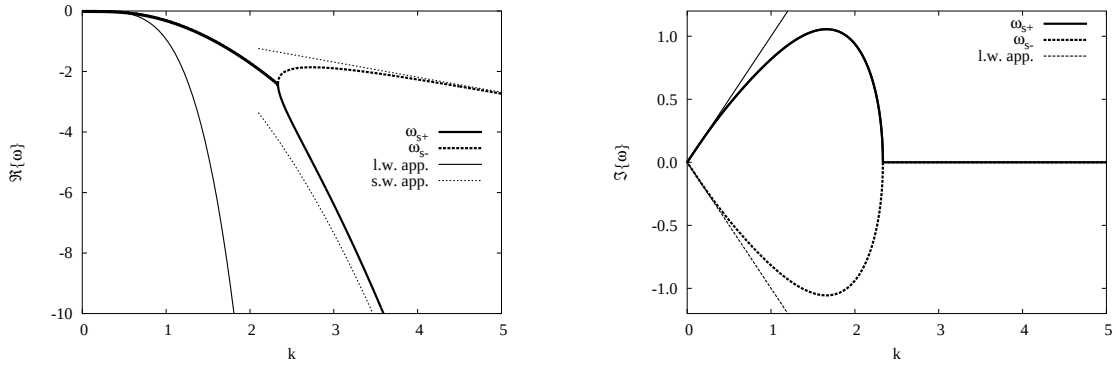

Figure 7: Sinuous soft branches for $\Gamma = 1$: Real part $\Re(\omega)$ (a), Imaginary part $\Im(\omega)$ (b). "l.w.app.": long wave approximation, "s.w.app.": short wave approximation.

The long wave asymptotic expansion of the sinuous soft branches $\omega_{s\pm}$ has been extended here to higher orders as compared to ref. [13], by using the symbolic algebra software MAPLE. For illustration, terms of the expansion are presented here up to $O(k^9)$:

$$\omega_{s\pm}(k) = -\left(\frac{2}{3}+\frac{4}{15}\,\Gamma^2\right)\,k^4+\left(\frac{6}{5}+\frac{304}{315}\,\Gamma^2+\frac{124}{2835}\,\Gamma^4\right)\,k^6$$
$$-\left(\frac{788}{315}+\frac{44948}{14175}\,\Gamma^2+\frac{7108}{17325}\,\Gamma^4\frac{43688}{6081075}\,\Gamma^6\right)\,k^8 \qquad (12)$$
$$\pm i\,\Gamma\left\{k-\frac{1}{2}k^3+\left(\frac{133}{120}+\frac{34}{315}\,\Gamma^2\right)\,k^5-\left(\frac{2}{9\,\Gamma^2}+\frac{2587}{1008}+\frac{1889}{2835}\,\Gamma^2+\frac{2764}{155925}\,\Gamma^4\right)\,k^7\right. .$$

In the range $0 < k < 0.5$ the quality of approximation of the soft spectrum by the asymptotic expansion improves with increasing truncation order in the range of orders considered. For $O(k^{17})$ the accuracy is even well below 0.5% for $k < 0.4$, cf. [1]. It, however, happens for any fixed value of k, that the accuracy of approximation increases for a while with increasing order of truncation, but then *decreases* with further increase of the order. This is typical for semiconvergent

(asymptotic) expansions. For large wave numbers, $k \to \infty$, the highest order with nonzero real part in the truncated expansion dominates the absorption, so that the (alternating) expansion has to be truncated at an order with negative real coefficient.

The difference in quality between the long wave approximation of the varicose and sinuous soft branches has also consequences for the numerical evaluation of eq. (7) for sinuous perturbations. In [3] it has been noticed that for sinuous perturbations the restriction to the leading order long wave approximation of the soft branches, eq. (10), instead of the exact dispersion relation yields a rather poor approximation of the response amplitude for localized perturbations, in contrast to the good approximation for varicose perturbations, to this order. However, if a pressure distribution with a larger spatial extension a is considered, the exponential decay of (the Fourier transform of) $f_0(\vec{X}, a)$ in the integrand of eq. (7) cuts off the influence of the short waves, due to the stronger localization (width $\propto 1/a$) of the shape function in the wave number space, and so a better approximation of the response by the long wave modes is to be expected. Fig. 8 shows, for $f_0(\vec{X}, 10)$, a comparison of the sinuous response amplitudes using the exact dispersion function (3) and the long wave approximation, at different approximation orders [13] of $\omega_{s\pm}(k)$. The long wave approximation up to $O(k^{13})$ exhibits an oscillatory behaviour to the left of the major wave trough and crest for $x < 1000$, cf. Fig. 8 (a)–(c), which is due to the dispersive terms of $O(k^3)$. This behaviour is not present, in this strength, in the numerical evaluation of the exact signal (7). However, the higher order approximation gives a significantly better approximation at large distances, $x \gg 1000$, compared with the leading order, eq. (10), cf. Fig. 8 (d).

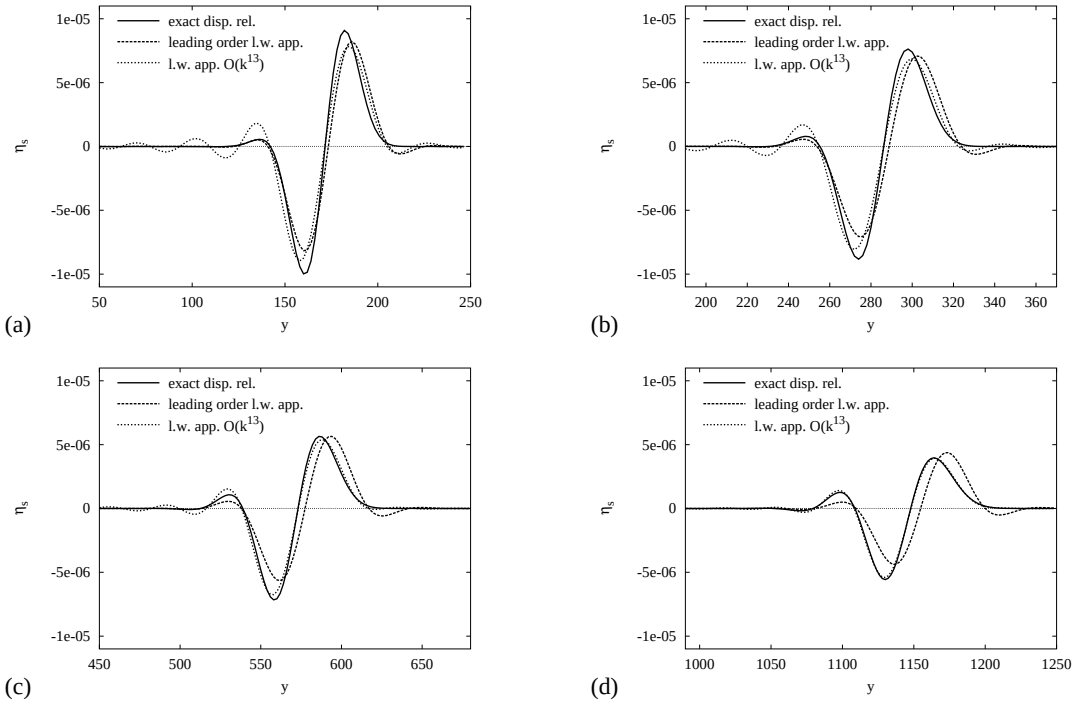

Figure 8: Disturbance amplitude $\eta_s(x, y)$ (in the rest frame of the disturbance source) of the sinuous disturbance along the (transverse) y–direction, at different distances x from the source, for $\Gamma = 10, V = 2\Gamma$: $x = 300$ (a), $x = 500$ (b), $x = 1000$ (c), $x = 2000$ (d).

Fig. 9 shows, for illustration, the response of the sheet to sinuous (a) and varicose (b) disturbances with the shape function $f_0(\vec{X}, 1)$ and with $V = 2\Gamma$, for $\Gamma = 1$ and $\Gamma = 10$, respectively. With increasing Γ, i.e. with increasing characteristic phase speed c_{ph}, the deflection amplitude of the response for both modes becomes increasingly oscillatory ahead of the moving pressure distur-

bance. Sinuous pressure perturbations cause almost straight wave crests that enclose a wedge shaped area in the wake of the disturbance with very small amplitude. This wedge corresponds to a twodimensional Mach cone of opening half angle $\theta = \sin^{-1} \Gamma/V$, caused in a nondispersive medium by a pointlike disturbance source moving faster than the phase speed $c_{ph} = \Gamma$.

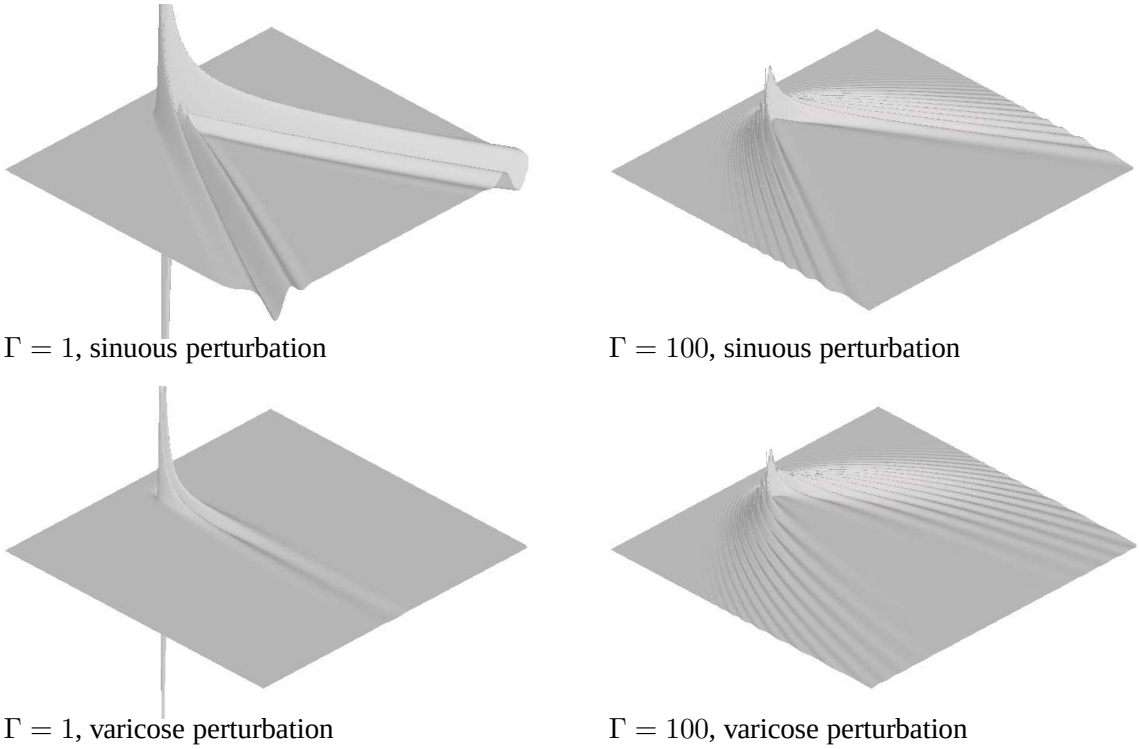

$\Gamma = 1$, sinuous perturbation

$\Gamma = 100$, sinuous perturbation

$\Gamma = 1$, varicose perturbation

$\Gamma = 100$, varicose perturbation

Figure 9: Propagation of disturbances for the shape function $f_0(\vec{X}, 1)$, $V = 2\Gamma$ (rest frame of disturbance): Numerical results for exact dispersion relations for sinuous perturbation and varicose perturbation.

4 Conclusions

The linear response of a viscous liquid sheet to moving persistent pressure disturbances has been investigated. The response to sinuous and varicose excitations, obtained by the Fourier–Laplace technique, has been presented in terms of an integral representation for the surface deflection amplitude of the sheet. The response signal is determined by the shape of the perturbing source, on the one hand, and by the structure of the spectral functions $D_{s,v}(k, \omega)$ of the sheet, on the other hand. The varicose and sinuous parts of the sheet spectrum consist of infinitely many hard branches $\omega_{v,s\alpha}(k)$ and of two soft branches $\omega_{v,s\pm}(k)$, which dominate the response of the sheet in the long time limit. The response amplitude to a steady excitation becomes in this limit stationary in a reference frame moving with the perturbation source and can be expressed as a twodimensional Fourier integral. This integral has been evaluated numerically, in its exact form and in an asymptotic approximation.

For varicose perturbations the exact signal has been compared with an analytic form obtained in the frame of the lowest order long wave approximation [4], showing good agreement for larger distances from the source. The response to sinuous disturbances encloses a wedge shaped region with very small amplitude, similar to a Mach cone. Its opening angle is determined by the speed ratio $c_{ph}/V = \Gamma/V$. The velocity Γ, showing up in it, keeps significance far beyond small (linear)

perturbations: it plays a key role even in the highly nonlinear process of edge retraction on a plane viscous sheet, cf. [2, 14].

5 Acknowledgement

This work has been supported by the German Research Foundation (DFG).

References

[1] N. Alleborn and H. Raszillier. Numerical investigation of the linear response of a viscous liquid sheet. In preparation for publication, 2005.

[2] N. Alleborn, F. Durst, and H. Lienhart. Use of curtain coating for surface treatment of concrete construction parts (in German). *Chemie Ingenieur Technik*, 77:84–89, 2005.

[3] N. Alleborn and H. Raszillier. Linear response of a viscous liquid sheet. In W. Gutkowski and T.A. Kowalewski, editors, *21st International Congress of Theoretical and Applied Mechanics — ICTAM04, Abstract Book and CD–Rom Proceedings*. Published by IPPT PAN, 15–21 August 2004.

[4] N. Alleborn and H. Raszillier. Linear response of a viscous liquid sheet to oscillatory external pressure perturbation in the long wave approximation. Varicose excitation. *Acta Mechanica*, 170:77–119, 2004.

[5] N. Alleborn and H. Raszillier. Propagation of disturbances in thin viscous liquid sheets. In *10th International Coating Science and Technology Symposium — Final Program and Extended Abstracts*, pages 40–43. ISCST — International Society of Coating Science and Technology, Newark, Scottsdale, Arizona, 25–27 September 2000.

[6] N. Alleborn, H. Raszillier, and F. Durst. Linear stability of non–Newtonian annular liquid sheets. *Acta Mechanica*, 137:33–42, 1999.

[7] J. Berntsen, T.O. Espelid, and A. Genz. An adaptive algorithm for the approximate calculation of multiple integrals. *ACM Trans. Math. Softw.*, 17:437–451, 1991.

[8] L. De Luca and M. Costa. Stationary waves on plane liquid sheets falling vertically. *Eur. J. Mech. B/Fluids*, 16:75–88, 1997.

[9] S. P. Lin. Stability of a viscous liquid curtain. *J. Fluid Mech.*, 104:111–118, 1981.

[10] S. P. Lin, Z. W. Lian, and B. J. Creighton. Absolute and convective instability of a liquid sheet. *J. Fluid Mech.*, 220:673–689, 1990.

[11] S. P. Lin and G. Roberts. Waves in a viscous liquid curtain. *J. Fluid Mech.*, 112:443–458, 1981.

[12] H. Raszillier. Liquid film coating — modelling and computation. In H.A. Mang, F.G. Rammerstorfer, and J. Eberhardsteiner, editors, *WCCM V – Fifth World Congress on Computational Mechanics*, Vienna, July 7–12, 2002.

[13] H. Raszillier. Linear response of a viscous liquid sheet to external pressure perturbation. long wave approximations. *Z. angew. Math. Phys.*, 56:59–91, 2005.

[14] G. Sünderhauf, H. Raszillier, and F. Durst. The retraction of the edge of a planar liquid sheet. *Phys. Fluids*, 14:198–208, 2002.